Effect of Hydrodynamic Shear Stress on Biofilm Adhesion to Organosilane Self-Assembled Monolayers on Titanium

Rebecca M. Lennen, Robert A. Brizzolara
Biological Sciences Group
Naval Surface Warfare Center, Carderock Division
9500 MacArthur Blvd.
West Bethesda, MD 20817-5700

I. Formation and optimization of organosilane self-assembled monolayers (SAMs) on titanium

INTRODUCTION

Derivitization of silica surfaces using organosilane precursors has been established for many years.[1,2,3] Extension to engineering materials would potentially be of great value. Potential applications include biological fouling (biofouling) control, increased or lowered adhesion, improved tribology, imparting antimicrobial properties, or inhibition of bacterial colonization that results in infections in medical implants. In particular, bacterial biofouling and the ultimate formation of biofilms in cooling systems on maritime vessels is a chronic and costly problem, which results in higher operating temperatures and decreased machinery and propulsion efficiency. This problem is exacerbated by the increasing use of titanium in heat exchangers in Naval vessels, which is more prone to biofouling than more traditional copper-nickel systems. Chlorination is commonly used for bacterial biofouling control in seawater piping systems and heat exchangers; however, environmental regulations on chlorine discharges are forcing alternative approaches to be considered. Ideally, such an approach would be capable of controlling biofouling in a cost-effective way without resulting in the storage or discharge of hazardous chemicals.

A possible approach is the derivitization of heat transfer surfaces to reduce biofouling adhesion. These surfaces cannot be treated with traditional nonfouling coatings due to the unacceptable increase of the overall heat transfer coefficient as a result of the thickness of these coatings. The use of extremely thin, nanoscale coatings that decrease bacterial biofouling adhesion would allow the biofilm to be removed by hydrodynamic wall shear due to normal water flow or a high velocity flush.

Organosilanes spontaneously self-assemble on hydroxylated surfaces, providing a strong, covalent attachment and a high areal density of desired functional groups. The native oxide on titanium, under ambient conditions, provides 2.6 hydroxyl groups per nm^2.[4] The mechanism of reaction is shown in Figure 1.[5] The precursor is an organosilane with the general formula $RSi(X_n)(CH_3)_{3-n}$, where R is an organic functional group and X is a chloride or alkoxy group. Only precursors with n=3 are considered here, due to their ability to form crosslinked surface networks. The X group is first hydrolyzed by residual water, either in solution or adsorbed on the surface, to form a silanol. The silanol then condenses by hydrogen bonding with hydroxyl groups on the surface, and spontaneous dehydration results in the formation of covalent bonds. A brief cure at elevated temperature is believed to assist in the crosslinking reaction between neighboring molecules.[2] After sufficient reaction time, a self-assembled monolayer (SAM) is formed, ideally with R groups extending away from the surface, thereby modifying surface chemical properties. Numerous procedures and

applications for the formation of organosilane SAMs on silica are given in the literature.[1,2,3,6,7] A few other reports focused on titanium metal or titania, including trichlorosilanes and trialkoxysilanes with amino, glycidoxy, and mercapto terminal groups on short alkyl chains; vinyl groups; and short and long chain alkyls.[8,9,10,11,12,13,14,15,16]

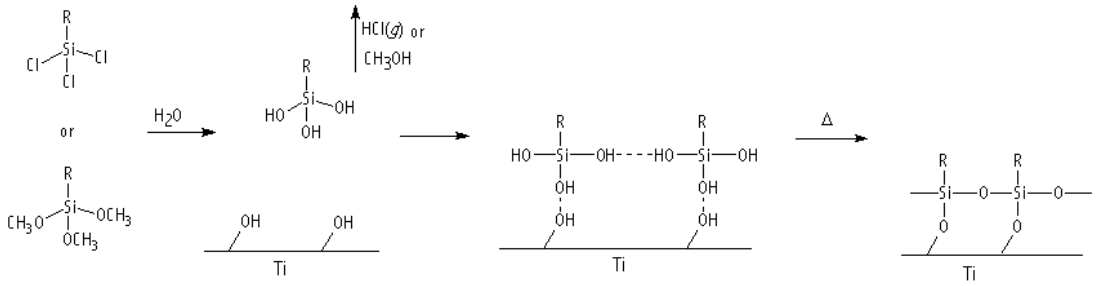

Figure 1. Mechanism of formation of self-assembled monolayers from organosilane precursors. A typical procedure involves dipping a clean substrate into a dilute solution of the organosilane precursor in an organic solvent. Small amounts of water in solution or adsorbed on the substrate surface assist the reaction. The final SAM derivatizes the substrate with a high areal density of oriented R groups.

In this paper, we report the attachment of organosilane precursors with a wide range of terminal functional R groups to the native oxide surface of titanium, with optimum reaction variables reported for several precursors. Terminal R groups used include alkyl chains, $CH_3(CH_2)_nSiCl_3$, with n=9, 11, or 15; a perfluorinated alkyl chain, $CF_3(CF_2)_5(CH_2)_2SiCl_3$; a trifluoromethyl group on a short alkyl chain, $CF_3(CH_2)_2SiCl_3$; a chlorine on a short alkyl chain group, $Cl(CH_2)_3SiCl_3$; an amino group on a short alkyl chain, $H_2N(CH_2)_3Si(OCH_2CH_3)_3$; a mercapto group on a short alkyl chain, $HS(CH_2)_3Si(OCH_2CH_3)_3$; and a vinyl group on a medium alkyl chain, $H_2C{=}CH(CH_2)_6SiCl_3$.

EXPERIMENTAL

Materials. Titanium foil, 99.99+%, 0.127 mm thick, was purchased from Alfa Aesar (Ward Hill, MA). Deionized water was obtained from a () system. n-Hexadecyltrichlorosilane (HTS), n-dodecyltrichlorosilane (DoTS), n-decyltrichlorosilane (DTS), 3-chloropropyltrichlorosilane (3Cl), and 8-octenyltrichlorosilane (OTS) were purchased from United Chemical Technologies (Bristol, PA). 1H,1H,2H,2H-perfluorooctyltrichlorosilane (13F) was purchased from Lancaster Synthesis, Inc. (Windham, NH) and from Gelest, Inc. (Morrisville, PA). 3,3,3-trifluoropropyltrichlorosilane (3F) was purchased from Lancaster Synthesis. 3-mercaptopropyltriethoxysilane (MPTES) and 3-aminopropyltriethoxysilane (APTES), >95%, was purchased from Gelest. Isopropanol, Optima grade; and acetone, electronic or Optima grade; were purchased from Fisher Scientific (Pittsburgh, PA). Ethanol, HPLC/Spectrophotometric grade; ethylene glycol, 99.8% anhydrous; toluene, 99.8% anhydrous; and diiodomethane, 99% were purchased from Sigma-Aldrich (Milwaukee, WI). All solvents, reagents, and organosilanes were used as-received without further purification.

Substrate cleaning and preparation. Titanium foil was cut into coupons of approximately 1x1 cm^2 area for optimization purposes; adhesion test coupons were cut so that the area exposed to water flow was 4.5x5 cm^2. Coupons were then placed in a sonic bath for

1 h in a solution of manual wash Sparkleen detergent (Fisher, Pittsburgh, PA) in deionized water, rinsed in deionized water, sonicated for 1 h in acetone, and sonicated for 1 h in isopropanol. Substrates were then rinsed again in deionized water and immersed in boiling deionized water for 30 min, to assist in saturating surface hydroxyl groups.

Formation of self-assembled monolayers. Cleaned substrates were transferred from deionized water to isopropanol and dried under a stream of high-purity nitrogen immediately before use. In a dry air atmosphere of less than 2%, but more typically less than 0.5% relative humidity, the substrates were transferred into glass beakers or petri dishes containing an 0.005 M solution of organosilane, for trichlorosilanes, or 1% (w/v) organosilane, for trialkoxysilanes, in toluene. Immersion times of the substrate in the adsorbate solution were between 5 min. and 24 h. After silanization, the substrates were removed from the adsorbate solution and rinsed consecutively in toluene and isopropanol. After the isopropanol rinse, the substrates were dried under high-purity nitrogen. No more than 2 hours after silanization, substrates were oven cured for 5 min. at 120°C.

Contact angle measurements. Contact angle measurements were taken between 1 day to a week after silanization. Contact angles were determined from sessile drops using a KSV Instruments CAM 100 optical contact angle viewer with some CAM 200 software capabilities. The drops are backlit by a red LED. The CAM 100/200 software captures the drop silhouette with a USB video camera and fits the contour to the Young-Laplace equation, determining the contact angles on each side of the drop at a user-set baseline. The black/white filtered image of the drop silhouette was thresholded as needed for each individual image. The volume of each drop was approximately 1 μL but was not precisely controlled. Drops were applied by first forming a pendant drop on the syringe tip, and then raising the platform on which the substrate laid until it just contacted the drop. The platform was then lowered to remove the syringe tip from the drop, and the drop image was immediately recorded. This was repeated to obtain a minimum of 6 contact angles, one on each side of the drop, from at least 3 drops for each liquid on each sample.

Surface free energy calculations. Surface free energies were calculated based on Lifshitz-van der Waals acid base component theory described by Van Oss, et al. This method splits the forces acting at the interface into Lifshitz-van der Waals, containing the sum of London, Debye, and Keesom forces, and Lewis acid and base components.[17] Contact angles were taken with three liquids, with a maximum of one nonpolar liquid, in order to solve for the Lifshitz-van der Waals, Lewis acid, and Lewis base components of the surface free energy: deionized water, ethylene glycol, and diiodomethane.

X-ray photoelectron spectroscopy. XPS spectra were recorded using a Physical Electronics 5400 system with unmonochromatized Mg Kα radiation at 400 W (15 kV). The take-off angle was 45° with respect to the sample surface. Angle resolved spectra were recorded at take-off angles of 15°, 20°, 30°, 45°, and 70°. Survey scans covered a binding energy range of 0-1100 eV with a constant detector pass energy of 178.950 eV. High-resolution scans were recorded at a pass energy of 35.750 eV for relevant binding energy regions to determine chemical states. The spot size for all scans was 1 mm x 3 mm. Background subtraction, peak integration, and peak fitting were all accomplished with Phi Access software (Physical Electronics, Eden Prairie, MN). Peaks were referenced to the C 1s hydrocarbon component at 284.6 eV. Main chamber pressures during analysis were in the

10^{-8} to 10^{-9} torr range. The following peak area sensitivity factors were used for the atomic concentration calculations, as provided with Phi Access software: C 1s, 0.296; O 1s, 0.711; N 1s, 0.477; Si 2p, 0.339; Ti 2p, 2.001; F 1s, 1.000; Cl 2p, 0.891. XPS spectra were not taken for SAMs of 3F due to the observation of significant x-ray induced damage.

Layer thicknesses were determined using the C1s/CKVV peak area ratio, corrected for substrate Auger electron emission.[18,19] Fractional coverage was determined using the attenuation of the Ti2p peak relative to a clean titanium sample.[20] Inelastic mean free paths used in these calculations were obtained from NIST Database 71 from the TPP-2M model by Tanuma, Powell, and Penn.[21,22,23] Overlayers were assumed to be composed of only carbon, to facilitate application of the layer thickness model.

RESULTS

Several variables were optimized in order to produce organosilane SAMs with the highest degree of orientation and the most coverage. These included substrate preparation procedure, immersion time of the substrate in the organosilane solution, moisture content of the solvent and of the atmosphere, ambient temperature during silanization, and use of an elevated temperature cure after silanization.

Substrate preparation. It was found that immersion of substrates in 12 M HCl or 18 M H_2SO_4 for 1 h resulted in no significant change in the percentage of adventitious carbon, as determined by XPS. Treatment with 12 M HCl resulted in 28.0±3.8% C, with 18 M H_2SO_4 resulted in 25.2±0.1% C, and no treatment resulted in 27.7±5.0% C. Various durations of detergent and solvent sonication was also tested. It was found that lengthy sonications were prerequisite to obtaining low water contact angles. The selected sequence of 1 h sonication in Sparkleen detergent in deionized water, followed by 1 h sonication in acetone, 1 h sonication in isopropanol, and 30 min. immersion in boiling deionized water, was found to produce water contact angles between 0-10°.

Immersion time and temperature. It is important to determine the appropriate immersion time for substrates in solutions of each organosilane precursor. If the reaction time is too short, incomplete SAMs with low coverages will form; and if the reaction time is too long, the possibility becomes larger for adsorption of bulk solution polymerized precursor, which decreases SAM quality by decreasing the degree of orientation. Adsorption isotherms were investigated by plotting fractional coverage as a function of immersion time, with typical data taken after 10 min., 25 min., 40 min., 1 h, 2 h, and between 3 to 24 h immersion times. Adsorption isotherms will also vary depending on temperature. Two different temperatures were tested, due to the possibility of a solid phase transition temperature slightly below room temperature and dependent on the length of the R group, as suggested by Silberzan et al. and later investigated further by Brzoska et al.[3,24] Optimal immersion times were selected as 2 h for HTS, DoTS, DTS, 13F, MPTES, and ONTS; and 3 h for 3Cl. No adsorption isotherm was generated for APTES, as 2 h was the only immersion time tested. Additionally, no adsorption isotherm could be generated for 13F due to the large influence of the fluorine atoms on electron IMFP, however the C1s/CKVV ratio could be plotted as a function of immersion time in order to visualize when surface saturation occurred.

Atmospheric and solution moisture. Organosilane solutions are minutely sensitive to small changes in solution water content, whether already absorbed by the solvent or absorbed during the course of a reaction from the ambient atmosphere. Silanizations were performed both in ambient conditions of varying relative humidity and in a dry atmosphere room with a relative humidity of less than 1%. Table 1 presents atomic percentages determined by XPS for selected samples after 2 h immersion times of the substrate in the organosilane solution at two different relative humidities. Figure 2 demonstrates the relative degree of orientation of HTS coatings prepared under various reaction conditions, by plotting the C/Si ratio as a function of tilt angle. Tilt angle is here defined as the angle between the surface normal and the electron detector. There is greater surface sensitivity at low tilt angle and greater bulk substrate sensitivity at high tilt angle. Therefore the more oriented the coating overlayer, the greater the difference between the C/Si ratio at 15° and 70°, with the ratio at 15° being largest.

Table 1. Atomic concentrations, ratios, and water contact angles for 2 h immersions of titanium in HTS and 13F, and 3 h immersions in 3Cl. Humidities were either ambient (typically 30-40% R.H.) or reduced (< 0.1% R.H.). The water sensitivity of trichlorosilane solutions is demonstrated, with the order of highest to lowest sensitivity being 13F > HTS > 3Cl.

	atomic% from XPS						*atomic ratios*			
Organosilane precursor	C%	O%	Ti%	Si%	Cl%	F%	C/Si	C/X	X/Si	θ_{water}(°)
HTS, ambient humidity	57.51	30.66	8.92	2.92	-	-	19.7	-	-	109
HTS, < 0.1% humidity	40.79	41.83	15.21	2.17	-	-	18.8	-	-	113
3Cl, ambient humidity	24.70	50.86	11.87	7.43	5.13	-	3.3	4.81	0.69	75
3Cl, < 0.1% humidity	19.44	55.56	19.15	3.45	2.40	-	5.6	8.10	0.70	73
13F, ambient humidity	31.63	7.16	0.29	3.74	-	57.19	8.5	0.55	15.3	115
13F, < 0.1% humidity	22.76	25.70	9.08	1.91	-	40.55	11.9	0.56	21.2	119

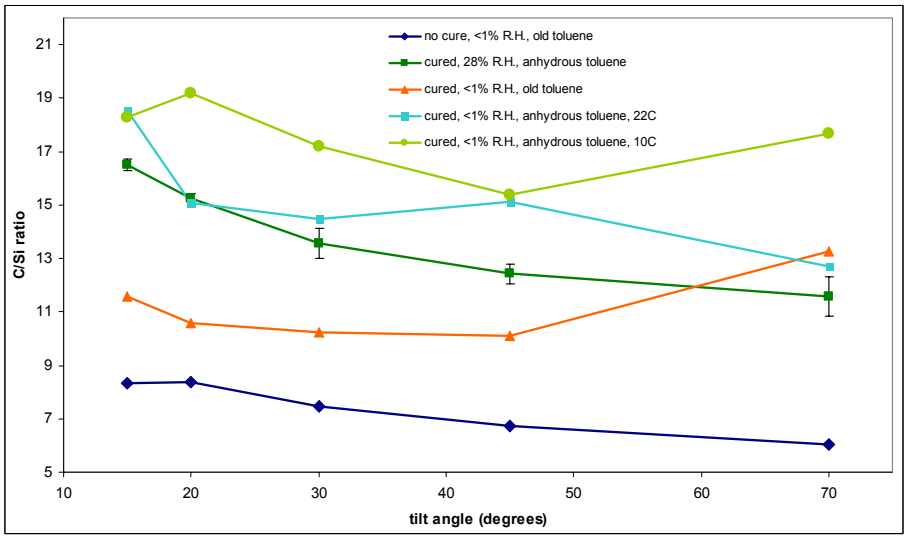

Figure 2. C/Si atomic ratios measured at different tilt angles for HTS on Ti, prepared with different reaction conditions: with or without a 120°C oven cure step following silanization, at two different relative humidities, with the use of water-saturated or fresh anhydrous toluene, and at temperatures of 22ºC or at a reduced temperature of 10ºC. Cured SAMs produced in a dry environment with anhydrous toluene at 22ºC had the highest degree of orientation and the largest C/Si ratios. Error bars are 95% confidence intervals about the mean.

Contact angles and solid surface tension. Contact angle measurements were taken on the organosilane coatings using three liquids for each termination: water, ethylene glycol or hexadecane, and diiodomethane. Contact angles, solid surface tension components, and solid surface tensions are presented in Table () for all selected optimal SAMs. Contact angles could also be plotted as a function of immersion time and temperature. Figure 3 depicts water contact angle and calculated solid surface tension data for HTS, DoTS, DTS, 3Cl, and 13F. Results were usually consistent with adsorption isotherms obtained by XPS.

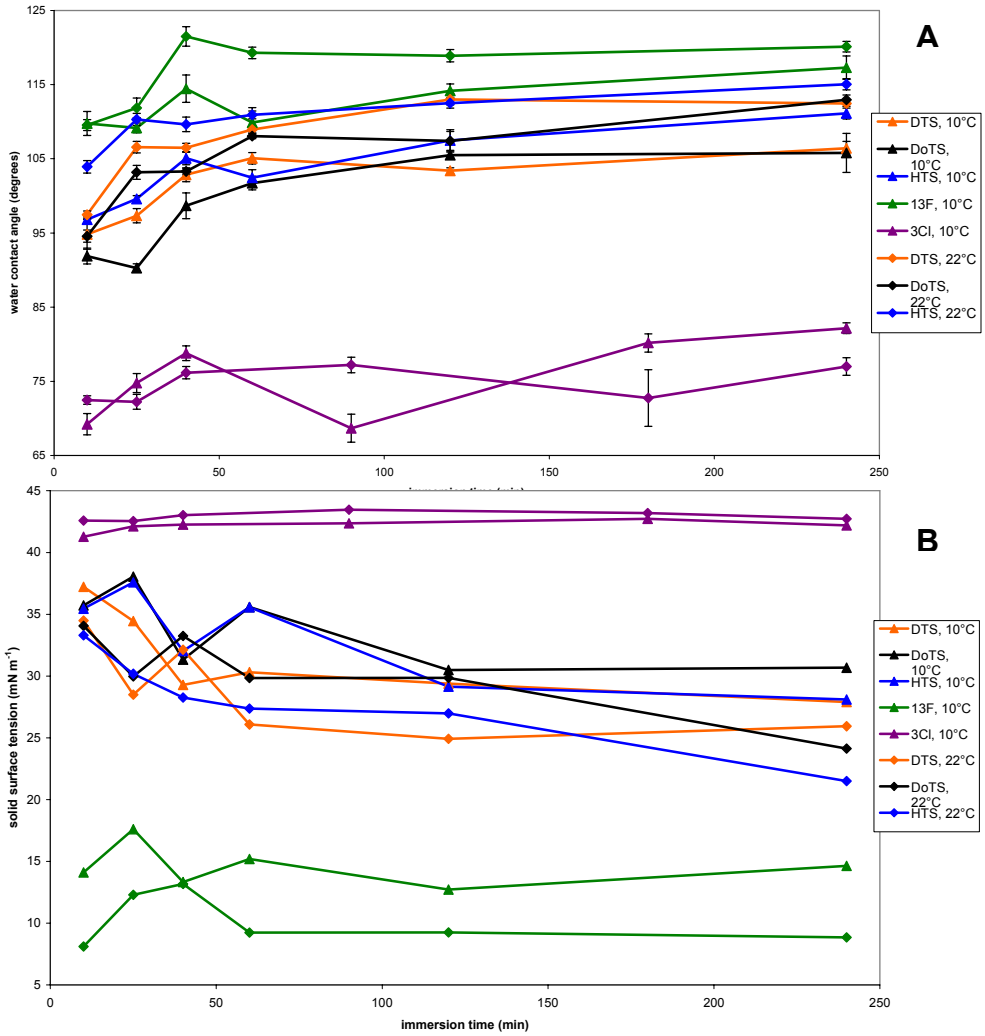

Figure 3. (A) water contact angles plotted against different immersion times of the Ti substrate in the organosilane solution, isotherms at 10°C and 22°C. (B) calculated solid surface tensions plotted against different immersion times of the Ti substrate in the organosilane solution, isotherms at 10°C and 22°C. On hydrophobic surface (DTS, DoTS, HTS, 13F), water contact angles are higher and solid surface tensions are lower when the reaction is performed at 22°C Error bars are 95% confidence intervals about the mean. Water contact angles and surface tensions level out between 1 h and 2 h immersion times.

XPS. XPS spectra were acquired of the various terminated samples in order to verify surface composition and to determine the relative degree of orientation between samples. Survey spectra of HTS, DoTS, DTS, 3Cl, 13F, MPTES, APTES, and OTS SAMs are shown

superimposed in Figure 4. ARXPS could also be used as a generic measure of coating orientation in SAMs composed of organosilanes with multiple atomic species. ARXPS of a

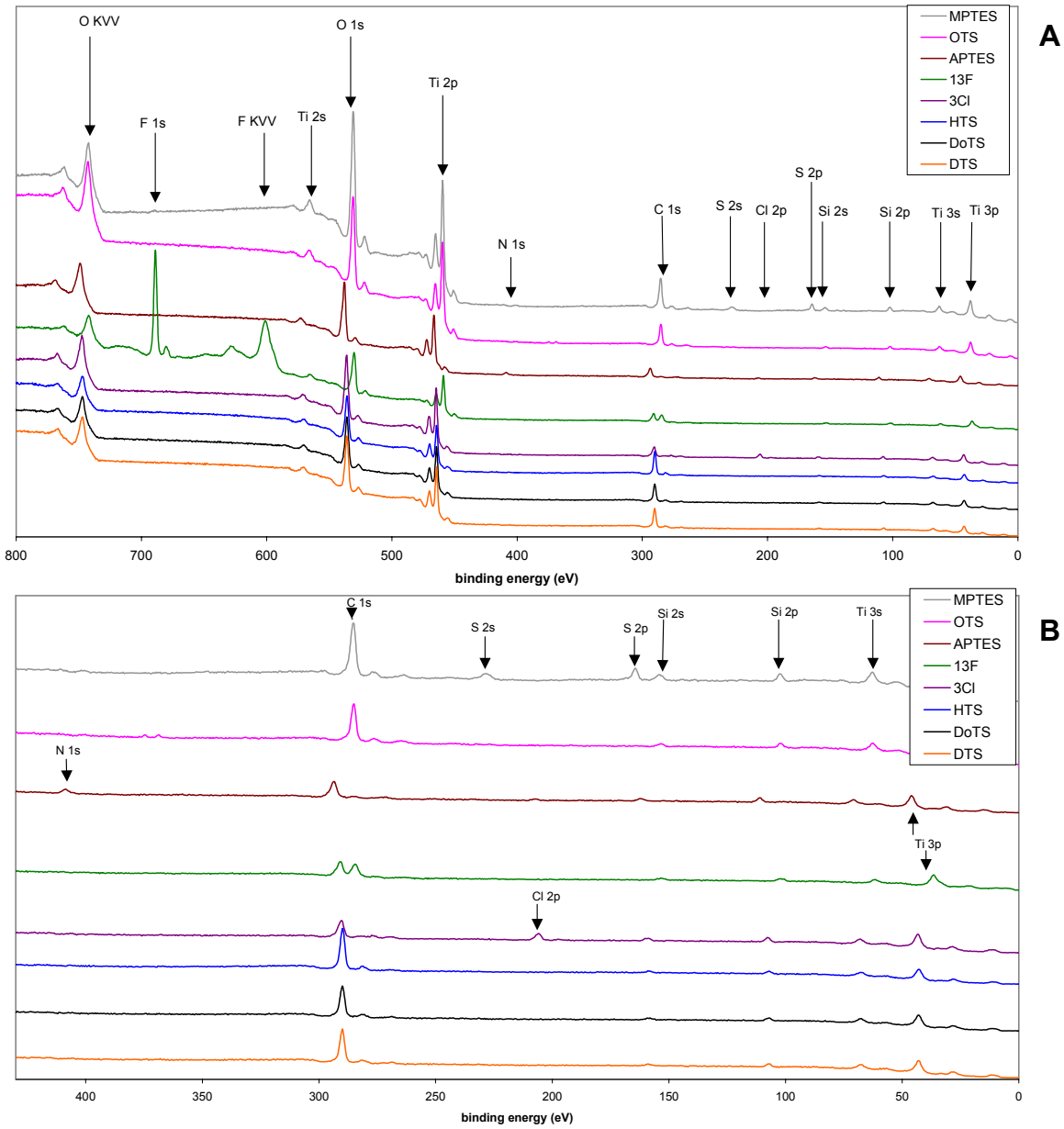

Figure 4. XPS survey spectra of SAMs of all organosilane precursors investigated, showing expected photoelectron and Auger electron peaks. Samples were 2 h immersions of titanium in the organosilane solutions, with less than 1% R.H. (3 h immersion for 3Cl, APTES and MPTES in ambient humidity). Spectra were not charge-corrected. (A) 0-800 eV binding energy range. (B) 0-430 eV binding energy range, showing details at lower energy.

13F SAM on titanium (2 h immersion time, dry atmosphere, 22°C) is shown in Figure 5. It is clear that both fluorine and carbon are oriented on top of silicon due to the decrease in the F/Si and C/Si ratios with increasing tilt angle (increasing sensitivity towards the substrate), and that fluorine and carbon are not oriented with respect to each other, due to no change in the F/C

ratio with increasing tilt angle. Compositions of all optimal SAMs and calculated layer thicknesses of non-fluorine containing SAMs are shown in Table 2.

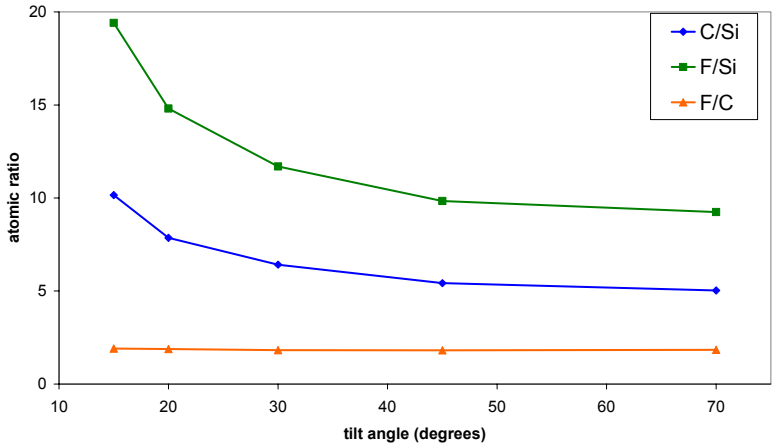

Figure 5. C/Si, F/Si, and F/C ratios as a function of tilt angle in a SAM of 13F on titanium (2 h immersion time, dry humidity, 22°C), determined by ARXPS. The decrease in C/Si and F/Si ratio with increasing tilt angle indicates the orientation of C and F atoms over Si atoms in the SAM. The constant value of the F/C ratio at all tilt angles indicates no orientation of F over C atoms.

Table 2. Atomic percentages (normalized to exclude the presence of small amounts of contaminating elements such as Na, N, and Ca), atomic ratios, water contact angles, and calculated solid surface tensions of selected optimal SAMs for each organosilane precursor. Optimal reaction conditions are discussed in the text. Molecular atomic ratios and solid surface tensions from the literature for each R group are reported in parentheses.[25,26,27,28,29,30] X represents Cl, F, N, or S, depending on the precursor. The formation of films of each organosilane on titanium are verified by the elemental compositions, changes in water contact angle, and calculated solid surface tensions.

organosilane precursor	*atomic% from XPS*								*atomic ratios*				
and R group	C%	O%	Ti%	Si%	Cl%	F%	N%	S%	C/Si	C/X	X/Si	θ_{water}(°)	γ_s (mN m^{-1})
DTS (-CH_3)	32.30	47.85	17.49	2.36	-	-	-	-	13.7 (10)	-	-	113 ± 1	24.9 (20)
DoTS (-CH_3)	32.33	47.92	17.19	2.55	-	-	-	-	12.7 (12)	-	-	107 ± 1	29.9 (20)
HTS (-CH_3)	40.79	41.83	15.21	2.17	-	-	-	-	18.8 (16)	-	-	112 ± 1	27.0 (20)
OTS (-CH=CH_2)	24.82	52.96	19.25	2.59	-	-	-	-	9.6 (8)	-	-	96 ± 1	33.1 (25-30)
3Cl (-CH_2Cl)	19.44	55.56	19.15	3.45	2.40	-	-	-	5.6 (3)	8.1 (3)	0.70 (1)	73 ± 4	43.2 (40-44)
13F (-CF_2CF_3)	22.76	25.70	9.08	1.91	-	40.55	-	-	11.9 (8)	0.56 (0.62)	21.2 (13)	119 ± 1	9.3 (6)
APTES (-CH_2NH_2) **	20.25	52.77	19.17	3.78	-	-	3.48	-	5.4 (3)	5.8 (3)	0.92 (1)	40 ± 0	42.0 (40)
MPTES (-CH_2SH)	25.04	53.56	16.48	2.49	-	-	-	2.42	10.1 (3)	10.3 (3)	0.97 (1)	29 ± 2	44

DISCUSSION

Silberzan et al. and Brzoska et al. observed an increase in critical surface tension as a function of temperature, with a critical temperature separating high-quality alkyltrichlorosilane SAMs on silicon wafer with lower surface tensions from lower quality SAMs with higher surface tension. Brzoska found a linear relationship between alkyl chain length and the threshold temperature between these two apparent phases. Our results in Figure 3 indicate the opposite, with higher quality SAMs formed at the higher temperature, which was above the

threshold temperature reported by Brzoska. A likely explanation for this discrepancy is atmospheric humidity, which varies with temperature if not otherwise controlled. The sensitivity of organosilane SAMs to atmospheric moisture during reaction is evident in Figure 2, where molecular orientation of HTS coatings are dramatically reduced when prepared at higher humidity, as well as in the elemental percentages in Table 1. Solutions of 13F in toluene are the most water sensitive. After less than 1 hour of exposure to a 30% R.H. atmosphere, clouding of the solution occurs, indicating the formation of polymer particles on the order of 100-1000 nm.

An elevated temperature cure following silanization also appears to assist in producing higher quality SAMs, as shown in Figure 2. Titanium silanized with HTS under otherwise identical reaction conditions with the exception of an elevated temperature cure exhibited a lower degree of orientation over cured samples.

Final selected reaction conditions for the formation of organosilane SAMs on titanium include: a very low ambient humidity that is preferably less than 1%, the use of an oven cure, and 2 hour immersion times of the substrate in the organosilane solution, with the exception of 3Cl for which 3 hours was optimal, likely due to the short chain length of this molecule.

II. Bacterial adhesion strength testing

INTRODUCTION

Biological fouling, or biofouling, begins when bacteria colonize a surface; the resulting biofilm is a dispersion of live and dead bacteria in a self-synthesized extracellular polysaccharide matrix. The first stage of bacterial colonization then facilitates colonization by eukaryotes, including protists, algae, bryozoans, tubeworms, barnacles, and mussels. Biofouling and its first stage of biofilm formation present serious problems related to three branches of transport phenomena in numerous industries and applications, including: (1) heat transport in cooling systems, due to the low thermal conductivity of biofilms of roughly 0.7 W/m-K;[31] (2) frictional losses, due to the viscoelastic behavior of biofilms;[32] and (3) mass transport issues, including the possibility of diffusive limitations that often prevent treatment of infectious biofilms with antibiotics.[33] Biofilms, and particularly biofilms on titanium, are implicated in bacterial infections, possibly due to the resistance of biofilms to both antibiotics and host immune defense.[34,35]

Many strategies have been implemented over the past few decades for controlling biofouling of surfaces. Particularly by the U.S. Navy, this includes chlorination of seawater piping systems and the use of copper ablative coatings or copper additives in ship hull paints. Due to environmental concerns and restrictions, so-called foul release coatings are being investigated as an alternative for hull biofouling. These coatings impart surface and/or mechanical properties, such as low elastic moduli and low surface tensions, to facilitate the detachment of biofouling under an applied shear stress.[36,37,38,39] However, traditional foul release coatings are bulk polymers by nature and could not be applied as an ultrathin coating for use in heat exchangers and cooling systems. Solid surface tension is a purely interfacial property that can be modified on the nanometer scale, therefore it would be beneficial to study the effect of modifying solid surface tension and investigating its impact on biofilm adhesion,

while holding all other material properties constant. Numerous previous studies have attempted to correlate surface tension with biofouling adhesion of hard-fouling invertebrates on bulk materials, resulting in a nonlinear correlation between adhesion and solid surface tension, often known as the "Baier curve".[40,41,42,43] This curve correlates biofouling adhesion with solid surface tension, with a distinct minimum corresponding to the surface tension of polydimethylsiloxane (PDMS) at 25 mN m^{-1}, with lower energy fluoropolymers exhibiting higher adhesion. Brady and Singer transformed the data to plots of adhesion vs. $(\gamma E)^{1/2}$, or the square root of the product of solid surface tension and elastic modulus, and found a nearly linear relationship.[44]

Most studies investigating bacterial adhesion or settlement on surfaces have focused on grafted oligo- or poly(ethylene glycol) functionalized SAMs or other biological inhibitory molecules.[45,46] Numerous studies have also focused on bacterial adhesion as a function of the hydrophobic or hydrophilic character of surfaces, although virtually all studies investigated only deposition, rather than adhesion strength. Wiencek and Fletcher prepared mixed alkanethiol SAMs of undecanethiol and and mercaptoundecanol to achieve a wide range of hydrophilic and hydrophobic surfaces, and observed a higher percent desorption of a *Pseudomonas* sp. on more hydrophilic SAMs under an imposed shear stress of 0.058 N m^{-2} over a 2 hour period.[47] Studies conducted with the marine diatom *Amphora coffeaeformis* var. *purpusilla*, and spores of the green algae *Enteromorpha linza*, found increased removal of the spores with decreasing solid surface tension after 5 minutes of exposure to a shear stress of 56 N m^{-2}, but decreased removal of diatoms with decreasing solid surface tension after 5 minute exposures to shear stresses of 1.9 and 9.2 N m^{-2}. It was suggested that this was due to the more hydrophobic extracellular polysaccharide produced by *Amphora*.[48]

This study investigates the adhesion strength of biofilms of *Pseudomonas fluorescens* to titanium modified with organosilane self-assembled monolayers, allowing the modification of surface tension while holding all other bulk material properties constant. Titanium is increasingly the material of construction of cooling systems on Naval vessels due to its corrosion resistance and high strength-to-weight ratio, and is also a common medical implant material due to its biocompatibility. It is hypothesized that bacterial biofilms will exhibit lower adhesion strength to low energy surfaces with low solid surface tension, and higher adhesion strength to high energy surfaces.

EXPERIMENTAL

Materials. All organosilane precursors, solvents, and contact angle fluids are previously described (Part I). Titanium foil, 0.025 mm thick, 99.94%, was purchased from Alfa Aesar (Ward Hill, MA).

Self-assembled monolayer preparation. The procedure for formation of organosilane self-assembled monolayers on titanium has been previously described (see Part I). Optimum reaction conditions were selected for SAM formation involving each precursor.

Bacterial cell culture. *Pseudomonas fluorescens* (ATCC 17552) was selected due to the prolific use of pseudomonads in biofilm and bacterial adhesion literature and due to its ability to form biofilms on surfaces of many different compositions.[49,50,51,52,53,54] Biofilm-forming phenotypes were selected for by immersing a flame-sterilized aluminum coupon in a

suspension of *P. fluorescens* in a medium of 5 g/L tryptic soy broth and 10 mM phosphate-buffered saline at room temperature on an agitator rotating at a low speed. Aluminum coupons were then removed from suspension and transferred to fresh medium every 2-5 days. Titanium coupons were rinsed in isopropanol, dried in an air stream, and immersed in medium containing a small piece of aluminum covered with biofilm. After 2-5 days, the titanium coupon was transferred to fresh medium. A picture of a biofilm coated coupon is shown in Figure 5.

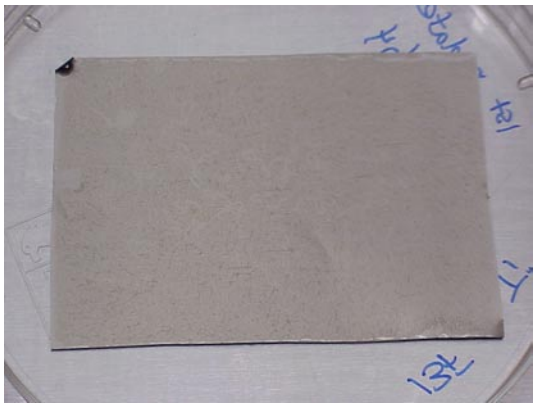

Figure 5. 13F coated titanium coupon covered with a 1-week old biofilm of Pseudomonas fluorescens.

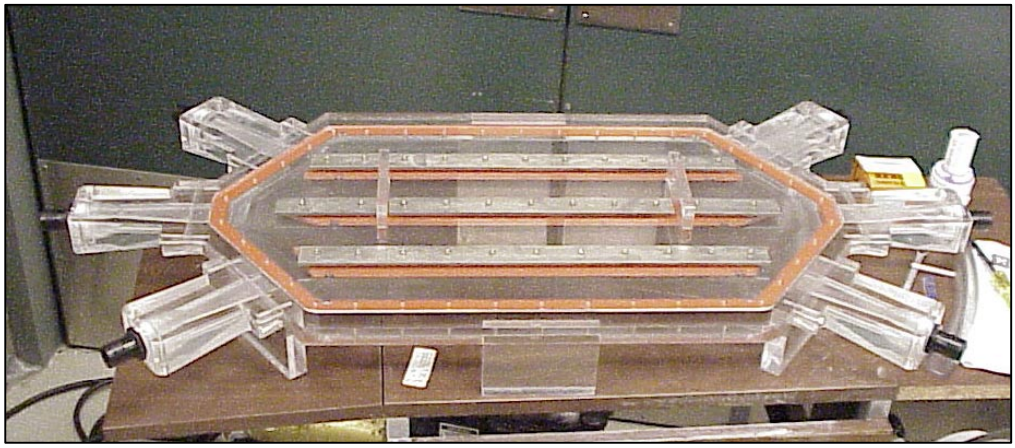

Figure 6. Turbulent flow cell for adhesion testing. Coupons are arranged in one of four channels and are held in place by silicone gasket on the channel dividers on the lid.

Turbulent flow cell. A turbulent flow cell was designed to provide a wide range of shear stresses quantifiable from the flow rate, Figure 6. Parallel-plate geometry was utilized, for which the shear stress can be estimated as

$$\tau_w = \frac{f\rho\overline{V}^2}{8} \tag{1}$$

where f is the friction factor, ρ is the fluid density, and $\overline{V}$ is the mean fluid velocity. This equation assumes a linear pressure profile, with fully-developed steady flow. The friction factor was solved for iteratively from the known flow rate using the Colebrook equation [55]

$$\frac{1}{f^{0.5}} = -2.0 \log\left(\frac{e/D}{3.7} + \frac{2.51}{\mathrm{Re}\, f^{0.5}}\right) \quad (2)$$

where e/D is the roughness and Re is the Reynolds number, with e/D set very close to zero for smooth walls. For calculation of Re, the hydraulic diameter, D_h=4A/P was utilized, where A is the cross-sectional area and P is the wetted perimeter of the flow channel.

Adhesion testing and biofilm quantification. After 1 week of biofilm growth on the modified or cleaned titanium, coupons were removed from suspension, rinsed gently in tap water to remove loosely adhered cells, and half of each coupon was immediately swabbed sequentially with 2 cotton-tipped swabs. Coupons were kept wet with tap water and quickly transferred into the flow cell apparatus. Flow exposure was for 5 minutes to 1 hour in tap water, depending on the flow rate, and immediately after the test, coupons were removed and the second half swabbed. Swab tips were immersed in 0.22 µm filter-sterilized 10 mM PBS and were vortexed vigorously. The resulting suspensions were then washed of extracellular protein by pelleting by centrifugation and resuspending by vortexing in 10 mM PBS three times, with cells from the two sequential swabs of each coupon half combined after the first resuspension. The final volume of cell suspension was 1.25 mL. Cells were then lysed with a Branson Sonifier 450 for three 20 s pulses at a power setting of 5 (20-25 W), while cooled in an ice-water bath, in order to release intracellular proteins. It was verified that these sonication settings resulted in 95% reduction in optical density at 600 nm, and a 98% reduction in CFU/mL in *P. fluorescens*. Portions of each cell suspension were then combined 1:1 or 2:15 with Coomassie Plus G-250 protein assay reagent. Absorbances were measured on a Hewlett Packard 8450A Diode Array Spectrophotometer at 595 nm and compared with a bovine serum albumin (BSA) standard curve of the appropriate concentration range. BSA absorbances vs. concentration curves were non-linear regressed to obtain the best cubic equation of fit, in order to correlate absorbances with protein concentrations in the unknowns. Protein concentrations were assumed to be representative of relative biofilm quantity and are reported in µg/mL of the lysed cell solution. Relative biofilm adhesion is reported as the percent reduction in protein concentration between the half of the coupon swabbed prior to flow exposure and the half of the coupon swabbed after flow exposure, with percentages averaged over many samples.

RESULTS

Solid surface tensions, water contact angles, and XPS atomic percentages measured specifically for organosilane coatings generated for adhesion testing are shown in Table 3.

Organosilane coatings derived from 13F, HTS, and 3Cl precursors were selected for testing due to the wide range of solid surface tensions tested. Cleaned uncoated titanium substrates were used as a negative control and represented a large solid surface tension approximately equal to that of water, based on contact angles measured previously (see Part I). Relative biofilm adhesion measured at flow rates of approximately 14 and 34 gallons per minute, corresponding to shear stresses of approximately 3.7 N m^{-2} with Re 9000, and 17.1 N m^{-2} with Re 21900 is shown in Figure 7. Exposure times to the 3.7 N m^{-2} and 17.1 N m^{-2} flows were 1 hour and 1 minute, respectively. These exposure times facilitated measurement of the percent change in total protein concentration within the detection limits of the assay.

Additionally, protein concentrations from cells swabbed off of coupons before flow exposure are included in Figure 7, representing a measure of relative biofilm accumulation on these surfaces after 1 week of growth.

Table 3. Averaged atomic percentages determined by XPS (normalized to exclude the presence of small amounts of contaminating elements such as Na, N, and Ca), atomic ratios, water contact angles, and calculated solid surface tensions for coated coupons and titanium controls tested.

organosilane precursor and R group	*atomic% from XPS*						*atomic ratios*				
	C%	O%	Ti%	Si%	Cl%	F%	C/Si	C/X	X/Si	θ_{water}(°)	γ_s (mN m^{-1})
HTS (-CH_3)	32.81	47.01	18.94	1.24	-	-	6.5 (16)	-	-	107	29.3
3Cl (-CH_2Cl)	19.15	54.97	21.37	2.89	1.65	-	6.6 (3)	11.6 (3)	0.57 (1)	64	39.9
13F (-CF_2CF_3)	19.78	36.14	15.06	1.10	-	27.95	18.0 (8)	1 (0.62)	25.4 (13)	108	17.5
Ti, uncoated	18.85	56.33	24.83	-	-	-	-	-	-	0-10	~72.8

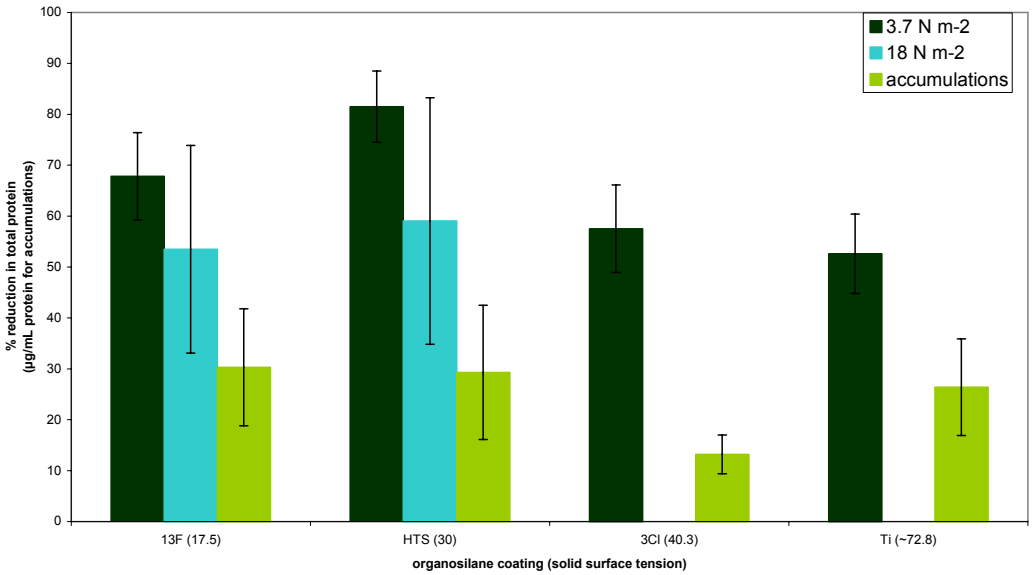

Figure 7. Percent reduction in total protein, used as a measure of relative biofilm adhesion, on coatings of 13F, HTS, 3Cl, and uncoated Ti control. Shear stresses of 3.7 N m^{-2} and 17.1 N m^{-2} were tested, with flow exposure times of 1 hour and 1 minute, for resolution considerations, respectively. Also shown on the same y-axis is the total protein concentration for swabbed biofilm prior to flow exposure, as a measure of relative biofilm accumulation. Error bars represent 95% confidence intervals about the mean. Error bars are large for 17.1 N m^{-2} data due to the small sampling size; measurements are still in progress.

DISCUSSION

As can be seen in Table 3, coating properties used in this study tended to exhibit lower coverages of organosilane than many of the optimal coatings presented in Part I. The reasons for this are unknown, however it is possible that there were variations in the water content of toluene in the organosilane solutions, considering that previously unopened anhydrous bottles were often immediately employed. However, the trend in surface tensions was still as

expected. In upcoming experiments, coatings will be produced in an atmosphere of approximately 1-2% relative humidity.

Examination of Figure 7 at 3.7 N m^{-2} indicates a stronger adhesion of the biofilm to the higher energy surfaces composed of 3Cl and Ti. However, examining the lower energy 13F and HTS coated surfaces, the biofilm appears to exhibit a slightly weaker adhesion on HTS, although the confidence intervals overlap. If the difference is real, this is in contradiction with our initial hypothesis. Due to the relatively poor coating quality, tests at 3.7 N m^{-2} are to be repeated with higher quality coatings in the future. Measurements at the higher shear stress of 18 N m^{-2} are still in progress. Preliminary data indicates no statistical difference in biofilm adhesion between 13F and HTS, although these measurements still represent small sample sizes.

Biofilm accumulation after 1 week of growth indicates no statistical preference of the cells towards 13F, HTS, or uncoated Ti. This lack of differential biofilm growth is not an unexpected result. *Pseudomonas* species attach to a surface via pili and/or flagella containing attractive moieties on their surfaces, and allowing the cell to initially adsorb to surfaces without direct surface-cell interactions.[56] Wild-type *Pseudomonas fluorescens* WCS365 has been shown to accumulate significantly to a variety of bulk polymers and glass, with two mutant strains showing defects in biofilm formation on hydrophobic surfaces and on polyvinylchloride.[49] However, cells in this study appear to accumulate to a lesser degree on 3Cl. The reasons for this are not yet clear and will be investigated further.

It would be fruitful in future investigations to study biofilm adhesion in *Pseudomonas fluorescens* 17552 wild-type and mutant strains deficient in pili or flagella, or in other species where initial adsorption occurs directly by interaction between the solid surface and cell surface. These initial results indicate that adhesion of a biofilm to titanium can be modified through the use of ultrathin organosilane coatings, with lower energy, hydrophobic coatings (13F and HTS) exhibiting increased biofilm removal under a hydrodynamic shear stress than higher energy, more hydrophilic surfaces (3Cl, and uncoated Ti). Additional tests could be performed on biofilms grown under higher initial shear conditions. It has been observed that biofilm morphology is influenced by the shear environment during growth, and that the shear stress required to initiate detachment in biofilms is directly proportional to the shear stress during growth.[32,57,58]

REFERENCES

1. Maoz, R.; Sagiv, J.; *J. Colloid Interface Sci.*, **100**, *465* (1984).
2. Wasserman, S. R.; Tao, Y.-T.; Whitesides, G. M.; *Langmuir*, **5**, 1074 (1989).
3. Silberzan, P.; Léger, L.; Ausserré, D.; Benattar, J. J.; *Langmuir*, **7**, 1647 (1991).
4. Simmons, G. W.; Beard, B. C.; *J. Phys. Chem.*, **91**, 1143 (1987).
5. Sagiv, J.; *J. Am. Chem. Soc.*, **102**, 92 (1980).
6. Vallant, T.; Brunner, H.; Mayer, U.; Hoffmann, H.; Leitner, T.; Resch, R.; Friedbacher, G.; *J. Phys. Chem. B*, **102**, 7190 (1998).
7. Stenger, D. A.; Georger, J. H.; Dulcey, C. S.; Hickman, J. J.; Rudolph, A. S.; Nielsen, T. B.; McCort, S. M.; Calvert, J. M.; *J. Am. Chem. Soc.*, **114**, 8435 (1992).
8. Sukenik, C. N.; Balachander, N.; Culp, L. A.; Lewandowska, K.; Merritt, K.; *J. Biomed. Mater. Res.*, **24**, 1307 (1990).

9. Xiao, S. J.; Textor, M.; Spencer, N. D.; Wieland, M.; Keller, B.; Sigrist, H.; *J. Mater. Sci.: Mater. Med.*, **8**, 867 (1997).
10. Wang, Y.; Supothina, S.; De Guire, M. R.; Heuer, A. H.; Collins, R.; Sukenik, C. N.; *Chem. Mater.*, **10**, 2135 (1998).
11. Cossement, D.; Delrue, Y.; Mekhalif, Z.; Delhalle, J.; Hevesi, L.; *Surf. Interface Anal.*, **30**, 56 (2000).
12. Mao, C.; Li, H.; Cui, F.; Feng, Q.; Wang, H.; Ma, C.; *J. Mater. Chem.*, **8**, 2795 (1998).
13. Laureyn, W.; Nelis, D.; Van Gerwen, P.; Baert, K.; Hermans, L.; Magnée, R.; Pireaux, J.-J.; Maes, G.; *Sensors and Actuators B*, **68**, 360 (2000).
14. Pursch, M.; Vanderhart, D. L.; Sander, L. C.; Gu, X.; Nguyen, T.; Wise, S. A.; Gajewski, D. A.; *J. Am. Chem. Soc.*, **122**, 6997 (2000).
15. Philippin, G.; Delhalle, J.; Mekhalif, Z.; *Appl. Surf. Sci.*, **212-213**, 530 (2003).
16. Lee, J. P.; Kim, H. K.; Park, C. R.; Park, G.; Kwak, H. T.; Koo, S. M.; Sung, M. M.; *J. Phys. Chem. B*, **107**, 8997 (2003).
17. Van Oss, C. J.; Good, R. J.; Chaudhury, M. K.; *J. Colloid Interface Sci.*, **111**, 378 (1986).
18. Ebel, M.; Schmid, M.; Ebel, H.; Vogel, A.; *J. Electron Spectrosc.*, **34**, 313 (1984).
19. Brizzolara, R. A.; Beard, B. C.; *Surf. Interface Anal.*, **27**, 716 (1999).
20. Briggs, D.; Seah, M. P.; *Practical Surface Analysis. Volume 1 – Auger and X-ray Photoelectron Spectroscopy*, 2nd ed. John Wiley & Sons: Chichester, UK. 1990.
21. Powell, C. J.; Jablonski, A.; *NIST Standard Reference Database 71: NIST Electron Inelastic-Mean-Free-Path Database*, Version 1.1, Dec. 2000.
22. Tanuma, S.; Powell, C. J.; Penn, D. R.; *Surf. Interface Anal.*, **21**, 165 (1994).
23. Tanuma, S.; Powell, C. J.; Penn, D. R.; *Surf. Interface Anal.*, **17**, 911 (1991).
24. Brzoska, J. B.; Ben Azouz, I.; Rondelez, F.; *Langmuir*, **10**, 4367 (1994).
25. Ulman, A.; *Ultrathin Organic Films*. Academic Press: Boston. 1991.
26. Bascom, W. D.; *Adv. Chem. Ser.* No. 87, 38 (1968).
27. Bascom, W. D.; *J. Colloid Interface Sci.*, **27**, 789 (1968).
28. Lee, L. Hn.; *Adv. Chem. Ser.*, No. 87, Sect. 8, 106 (1968).
29. Lee, L. Hn.; *J. Colloid Interface Sci.*, **27**, 751 (1968).
30. Park, S.-J.; Jin, J.-S.; Lee, J.-R.; *J. Adh. Sci. Technol.*, **14**, 1677 (2000).
31. Characklis, W. G.; Turakhia, M. H.; Zelver, N.; in *Biofilms*. eds. W. G. Characklis, K. C. Marshall. John Wiley & Sons: New York. 1990.
32. Stoodley, P.; Cargo, R.; Rupp, C. J.; Wilson, S.; Klapper, I.; *J. Ind. Microbiol. Biotechnol.*, **29**, 361 (2002).
33. Suci, P. A.; Vrany, J. D.; Mittelman, M. W.; *Biomaterials*, **19**, 327 (1998).
34. Gristina, A. G.; *Science*, **237**, 1588 (1987).
35. Barth, E.; Gristina, A. G.; *Biomaterials*, **10**, 525 (1989).
36. Griffith, J. R.; Bultman, J. D.; *Naval Engineers J.*, 129 (April, 1980).
37. Lindner, E.; *Biofouling*, **6**, 193 (1992).
38. Tsibouklis, J.; Stone, M.; Thorpe, A. A.; Graham, P.; Peters, V.; Heerlien, R.; Smith, J. R.; Green, K. L.; Nevell, T. G.; *Biomaterials*, **20**, 1229 (1999).
39. Thorpe, A. A.; Peters, V.; Smith, J. R.; Nevell, T. G.; Tsibouklis, J.; *J. Fluorine Chem.*, **104**, 37 (2000).
40. Baier, R. E.; DePalma, V. A.; in *Management of Occlusive Arterial Disease.* ed. W. A. Dale. Yearbook Medical Publishers: Chicago. 1971.
41. Brady, R. F.; Aronson, C. L.; *Biofouling*, **19**, 59 (2003).
42. Baier, R. E.; in *Adsorption of Microorganisms to Surfaces.* eds. G. Bittan, K. Marshall. Wiley Interscience Publishers: New York. (1980).

43. Fletcher, M.; Pringle, J. H.; *J. Colloid Interface Sci.*, **104**, 5 (1985).
44. Brady, R. F.; Singer, I. L.; *Biofouling*, **15**, 73 (2000).
45. Kingshott, P.; Wei, J.; Bagge-Ravn, D.; Gadegaard, N.; Gram, L.; *Langmuir*, **19**, 6912 (2003).
46. Qian, X.; Metallo, S. J.; Choi, I. S.; Wu, H.; Liang, M. N.; Whitesides, G. M.; *Anal. Chem.*, **74**, 1805 (2002).
47. Wiencek, K. M.; Fletcher, M.; *J. Bacteriol.*, **177**, 1959 (1995).
48. Finlay, J. A.; Callow, M. E.; Ista, L. K.; Lopez, G. P.; Callow, J. A.; *Integr. Comp. Biol.*, **42**, 1116 (2002).
49. O'Toole, G. A.; Kolter, R.; *Molec. Microbiol.*, **28**, 449 (1998).
50. Duddridge, J. E.; Kent, C. A.; Laws, J. F.; *Biotechnol. Bioeng.*, **24**, 153 (1982).
51. Wiencek, K. M.; Fletcher, M.; *J. Bacteriol.*, **177**, 1959 (1995).
52. Kingshott, P.; Wei, J.; Bagge-Ravn, D.; Gadegaard, N.; Gram, L.; *Langmuir*, **19**, 6921 (2003).
53. Wirtanen, G.; Alanko, T.; Mattila-Sandholm, T.; *Colloids and Interfaces B: Biointerfaces*, **5**, 319 (1996).
54. Medilanksi, E.; Kaufmann, K.; Wick, L. Y.; Wanner, O.; Harms, H.; *Biofouling*, **18**, 193 (2002).
55. Colebrook, C. F.; *J. Inst. Civil Eng., London*, **11**, 13 (1938-1939).
56. O'Toole, G. A.; Kolter, R.; *Molec. Microbiol.*, **30**, 295 (1998).
57. Stoodley, P.; Doyle, J. D.; Lappin-Scott, H. M.; "Influence of flow on the structure of bacterial biofilms", *Eighth International Symposium on Microbial Ecology*, Halifax, Nova Scotia, Canada. August 1998.
58. Purevdorj, B.; Costerton, J. W.; Stoodley, P.; *Appl. Env. Microbiol.*, **68**, 4457 (2002).